

Títol del treball:

**Tuning RAHB strength exciting from singlet to triplet state with
different topology of PAHs chains**

Estudiant: Maria Antonia Samaniego Recasens

Grau en Química

Correu electrònic: msamaniegorecasens@gmail.com

Tutor: Silvia Simon Rabaseda

Cotutor*:

Empresa / institució: Universitat de Girona

Vistiplau tutor (i cotutor*):

Nom del tutor: Silvia Simon Rabaseda

Nom del cotutor*:

Empresa / institució: Institut de Química Computacional i Catàlisi

Correu(s) electrònic(s): silvia.simon@udg.edu

*si hi ha un cotutor assignat

Index

Summary	2
Resumen	3
Resum	4
1 – Introduction	5
2- Objectives	8
3 – Methodology	9
4 – Sustainability	10
5 - Results and discussion	11
A. Adding RAHB:	11
B. Linear topology:	12
B.1. Linear trend (L1):	12
B.2. Linear topology for both isomers:	14
C. Kink structure for both isomers:	16
D. Combined topology:	18
6- Conclusions	21
7- Bibliography	22
8 -Supporting information	25

Summary

Resonance assisted hydrogen bond (RAHB) are one of the strongest non-covalent interactions. Resonance assists the hydrogen bond in the π -electron system. Between $-\text{CHO}$ group and $-\text{OH}$ it can be given an RAHB between the hydrogen of the $-\text{OH}$ group and the oxygen of the $-\text{CHO}$ group, this system will be called *quasi*-ring. Aromaticity and unpaired electrons in the triplet state may suffer changes if the RAHB is integrated to an aromatic ring.

In order to verify this, the *quasi*-ring was placed in different polycyclic aromatic hydrocarbons (PAHs) of different sizes and topologies. The structures analysed were linear and kink topologies; and also, they were classified by families (depending on the number of six-membered rings (6-MR) that PAHs have), the bigger family calculated was integrated by five 6-MR plus a *quasi*-ring. The bond distances of O--H and C=C of the RAHB and the excitation energy were calculated for all the compounds. Spin density distribution and aromaticity were analysed.

For the linear compounds, spin density distribution and aromaticity follow the same behaviour: as the chain lengthens the unpaired electrons locate in the middle part of the chain. The bond distances of the O--H and C=C for the S_0 are larger than the T_1 ; and as the chain gets longer the bond distances of T_1 increases until it gets a similar value as the S_0 . If the *quasi*-ring is not in the linear trend but in the next possible placement, the behaviour is similar; but, the T_1 is larger than the S_0 and for the spin density distribution there is light spin density at the oxygen atoms.

For kink compounds, spin density distribution and aromaticity follow a different behaviour than the linear compounds: the unpaired electrons locate in the *quasi*-ring, even if the chain lengthens. For the bond distances of O--H and C=C the S_0 and the T_1 states don't follow any behaviour as the chain lengthens.

To verify these statements, an analysis was made to a topology in which had a linear and kink stretch, and it was proved that for the linear stretch the behaviour was similar to the linear compounds; and for the kink stretch the behaviour was similar to the kink compounds. This is very interesting for future studies, as the bond distances can be tuned by changing the PAH topology.

Resumen

El enlace de hidrógeno asistido por resonancia (RAHB) es uno de los enlaces no covalentes más fuertes. La resonancia asiste al enlace de hidrógeno en el sistema de electrones π . Entre el grupo -CHO y -OH se da un RAHB entre el hidrógeno del grupo -OH y el oxígeno del grupo -CHO, este sistema se llama *quasi-ring*. La aromaticidad y los electrones no apareados en estado de triplete (T_1) pueden sufrir cambios si el RAHB se integra a un anillo aromático.

Para comprobarlo, el *quasi-ring* se ha colocado en diferentes hidrocarburos aromáticos policíclicos (PAH) de diferentes tamaños y topologías. Las estructuras analizadas son topologías lineales y de zigzag; y también se han clasificado por familias (según el número de anillos de seis miembros (6-MR) que tienen las PAH), la familia más grande está formada por cinco 6-MR más un *quasi-ring*. Se han calculado las distancias de enlace de O-H y C = C del RAHB y la energía de excitación para todos los compuestos. También, se ha analizado la distribución de la densidad de spin y la aromaticidad.

Para los compuestos lineales, la densidad de spin y la aromaticidad siguen el mismo comportamiento: a medida que la cadena se alarga los electrones no apareados se localizan en el centro de la cadena. Las distancias de enlace en el singlete (S_0) son mayores que en el T_1 ; y a medida que la cadena se alarga, las distancias de enlace de T_1 aumentan hasta obtener un valor similar al S_0 . Si el *quasi-ring* no se encuentra en la tendencia lineal, sino en la siguiente posición posible, el comportamiento es similar; sin embargo, el T_1 es mayor que el S_0 y en la distribución de la densidad de spin hay una leve densidad de spin en los átomos de oxígeno.

Para los compuestos zigzag, la densidad de spin y la aromaticidad siguen un comportamiento diferente que los compuestos lineales: los electrones no apareados se localizan en el *quasi-ring*, incluso cuando la cadena se alarga. Sobre las distancias de enlace, no siguen ninguna tendencia determinado a medida que la cadena se alarga.

Para verificar estas afirmaciones, se ha hecho un análisis más profundo de una topología que tenía un tramo lineal y uno de zigzag, y se ha demostrado que para el tramo lineal el comportamiento es similar al de los compuestos lineales; y para el tramo del zigzag el comportamiento es similar al de los compuestos de zigzag. Esto es muy interesante para futuros estudios, ya que se pueden tunear las distancias de enlace cambiando la topología del PAH.

Resum

L'enllaç d'hidrogen assistit per ressonància (RAHB) és una de les interaccions no covalents més fortes. La ressonància assisteix l'enllaç d'hidrogen en el sistema d'electrons π . Entre el grup $-CHO$ i $-OH$ es pot donar un RAHB entre l'hidrogen del grup $-OH$ i l'oxigen del grup $-CHO$, aquest sistema s'anomena *quasi-ring*. L'aromaticitat i els electrons no aparellats en estat de triplet (T_1) poden patir canvis si el RAHB s'integra a un anell aromàtic.

Per comprovar-ho, el *quasi-ring* s'ha col·locat en diferents hidrocarburs aromàtics policíclics (PAH) de diferents mides i topologies. S'han analitzat topologies lineals i de zig-zag; i també classificades per famílies (segons el nombre d'anells de sis membres (6-MR) que tenen les PAHs), la família més gran s'ha format per cinc 6-MR més un *quasi-ring*. S'han calculat les distàncies d'enllaç d'O-H i C = C del RAHB i l'energia d'excitació per a tots els compostos. També, s'ha analitzat la distribució de la densitat de spin i l'aromaticitat.

Per als compostos lineals, la densitat de spin i l'aromaticitat segueixen el mateix comportament: a mesura que la cadena s'allarga els electrons no aparellats es localitzen al centre de la cadena. Les distàncies d'enllaç per al singlet (S_0) són més grans que el T_1 ; i a mesura que la cadena s'allarga, les distàncies d'enllaç de T_1 augmenten fins a obtenir un valor similar al S_0 . Si el *quasi-ring* no es troba en la tendència lineal, sinó en la següent posició possible, el comportament és similar; però, el T_1 és més gran que el S_0 i per a la distribució de la densitat de spin hi ha una lleu densitat de spin als àtoms d'oxigen.

Per als compostos zig-zag, la densitat de spin i l'aromaticitat segueixen un comportament diferent que els compostos lineals: els electrons no aparellats es localitzen al *quasi-ring*, fins i tot quan la cadena s'allarga. Per a les distàncies d'enllaç d'O - H i C = C, els estats S_0 i T_1 no segueixen cap comportament determinat a mesura que la cadena s'allarga.

Per verificar aquests comportaments, s'ha fet un anàlisi més profund d'una topologia que tenia un tram lineal i un de zig-zag, i s'ha demostrat que per al tram lineal el comportament és similar als compostos lineals; i per al tram del zig-zag el comportament és similar als compostos de zig-zag. Això és molt interessant per a futurs estudis, ja que es poden ajustar les distàncies d'enllaç canviant la topologia dels PAHs.

1 – Introduction

Hydrogen bonds (HB) are one of the strongest non-covalent interactions. [1] One can find many HB with different strength. Resonance-assisted hydrogen bonds (RAHB) are one of them, being stronger than the conventional one. In that case, resonance assists the hydrogen bond by changing the elongation of hydrogen bond distance in the π electron system.[2, 3]

An example of this compound is malonaldehyde, it's a cyclic RAHB structure which contains six delocalized electrons. [2] The relation between H-bonds strength and the π -electron delocalization has been of a great interest. In that sense, adding an aromatic ring to the malonaldehyde will make the π -electrons less available, so it will change RAHB distance. There is a relationship between aromaticity and the RAHB integrated to an aromatic ring: if RAHB is integrated to an aromatic ring, this may effect the π -electron delocalization in the aromatic part of the compound. This is the case of hydroxybenzaldehyde (HA).

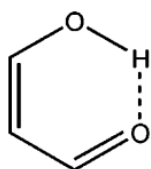


Figure 1. Malonaldehyde representation. Figure extracted from paper [2].

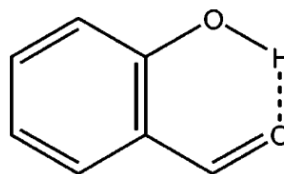


Figure 2. Hydroxybenzaldehyde representation. Figure extracted from paper [2]

Commonly RAHB is treated as a local effect, meaning that it has an impact only on the parts of the compound that are involved in this interaction. But, there are reports that postulate RAHB may have impact on electron distribution also in other areas of the compound. [4, 5]

In a recent paper by Pareras *et al* [1], there was found a relation between the intermolecular RAHB and the local aromaticity of 6-MRs (6-MR) to a series of *o*-hydroxyaryl aldehyde species. It was analyse how RAHB formation affected aromaticity in the adjacent 6-MR and how the different topology of the aromatic 6-MRs modify the strength of the RAHB fused to this aromatic ring.

Pareras *et al.* [1] showed that the HB strength of RAHB in different PAHs could be tuned by the topology of the fused PAHs chains:

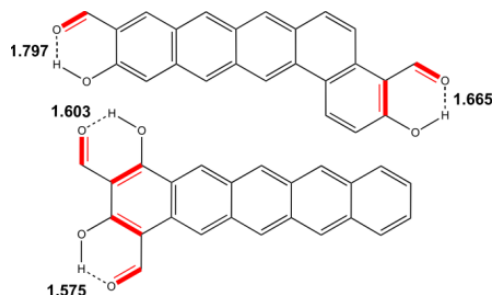


Figure 3. Different topologies show that depending of the placement of the RAHB the bond distance change. Images extracted from paper [1].

The idea of using aromaticity and antiaromaticity to change the singlet-triplet energy gap has been used in order to create new materials in the field of organic electronics, photoluminescence, photowitching and singlet-fission capable materials. One of the latest paper about these materials is [6] which was released months ago: “classes of aromatic molecules can be synthesized in extreme environments covering low temperatures in molecular clouds (10 K) and hydrocarbon-rich atmospheres of planets and their moons (35–150 K) to high-temperature environments like circumstellar envelopes of carbon-rich Asymptotic Giant Branch Stars stars and combustion systems at temperatures above 1400 K thus shedding light on the aromatic universe we live in.”

Aromaticity is a property which determines improved thermodynamic stability, changes in the bond length and special chemical reactivity. [7] “According to Hückel’s rule a planar conjugated monocycle is aromatic if it possesses $(4n + 2)$ π -electrons” “By contrast, planar cyclic, conjugated systems that possess $4n\pi$ -electrons are unstable, very reactive and have alternating single and double bonds; these are antiaromatic” [8] “Baird rule’s states that the aromatic nature of compound will reverse upon excitation from the singlet ground state to the first $\pi\pi^*$ triplet state.” Benzene is Hückel-aromatic in the ground state and Baird-antiaromatic in the $\pi\pi^*$ triplet excited state. In the past, aromaticity studies have centred on the ground state, but in recent times, the excited state has received more attention. Singlet state (S_0) is when all the electrons spins are paired in the molecular electronic state and triplet state (T_1) is when excitation transfer electrons into a higher energy level.[9]

Let’s focus first on the benzene. As it is well known the π delocalization on benzene can be described using the next Molecular Orbital diagram. π -orbitals are the responsables of the double bond and they show a delocalization character:

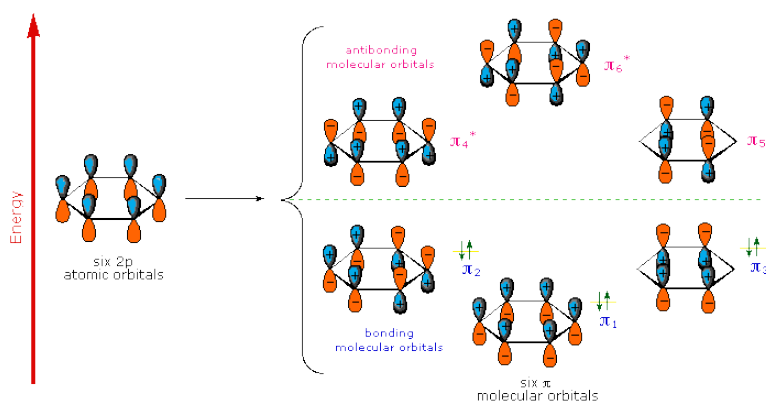


Figure 4. Molecular orbitals of benzene and its S_0 extracted from paper [10].

When benzene is excited to its T_1 state the unpaired electrons can be seen using the spin representation. The total spin density distribution is the difference between α and β -spin distributions and shows the distribution of unpaired electron. Spin density distribution in benzene in its T_1 is shown in **Figure 5**. The benzene has excitation energy of 3.8 eV. (calculated by B3LYP/6-31++G)).

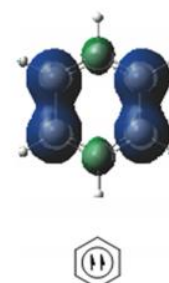


Figure 5. Spin density distribution of benzene in its T_1 extracted from paper [7].

In a recent paper by *Markert et al.* [8] they carried out a study to predict the spin distribution in different polycyclic aromatic hydrocarbons (PAHs) of different sizes and topologies. They analysed different structures motifs, it can be seen in **figure 6**. Each of these topologies present a different behaviour related to spin densities. It was concluded that for larger polycyclic molecules the spin density would accumulated in the center rings for lineal compounds or in the longer linear stretch of the compound.

It was concluded that “Spin will accumulate in the center ring(s) of a linear (L) subunit. When more than one L subunit is present, the spin will accumulate in the longer linear stretch and/or in the one that has least overlap with angular (A) subunits. When no L subunit is present, the tetracyclic subunits (C/Z motifs) of the compound determine the location of the spin. The preference is for the Z motif. When there are two identical (i.e., equivalent) motifs that share highest priority (e.g., identical L or Z subunits), symmetry can be broken and the spin will accumulate on one of the motifs.”[8]

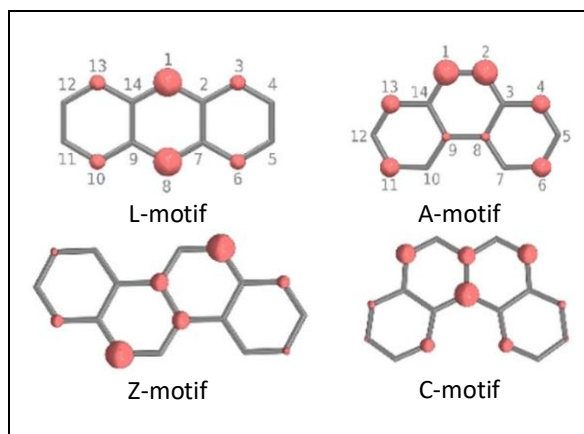


Figure 6. Spin density distribution for each motif studied in paper [7].

2- Objectives

The aim of this work is to analyse how the RAHB distances behave when it is excited in its triplet state. At the same time it will be analysed the change in HB distances, singlet-triplet state energy difference (gap S-T) and aromaticity for different topologies of fused PAHs.

In first place, we studied linear and kink structures and how adding more 6-MRs and their respective isomers were affecting the gap S-T, spin density and aromaticity. Then, we classified a variety of possible structures into five families. Family 1 is formed by a 6-MR and a quasi-ring; Family 2 is formed by two 6-MRs and a quasi-ring; family 3 is formed by three 6-MRs and a quasi-ring; family 4 is formed by four 6-MRs and a quasi-ring; and family 5 is formed by five 6-MRs and a quasi-ring.

The affectation of elongation of hydrogen bond and spin density in the singlet and the triplet state was studied in all the compounds. Aromaticity was studied in linear and kink structure.

3 – Methodology

Geometries of all compounds were optimized using DFT methods in the Gaussian 16 [11] set of codes. The B3LYP functional [12, 13, 14, 15] was applied in conjunction with the 6-311 +G (d,p)[16, 17] basis set for all atoms. The frequency was analysed to verify that the optimized geometries correspond to a minima in the potential energy surface. All structures were planar.

In order to calculate the aromaticity the ESI-3D program [18, 19, 20] was used. There are many parameters to define the aromaticity within a molecule. Some of them are based in energetic parameters, others are more related to geometry, and others to electronic density. When electronic parameters are considered, one can defined the aromaticity in terms of delocalization index. A delocalization index ($\delta(A, B)$) is defined as the amount of electron pairs between two atoms A and B [1]:

$$\delta(A, B) = 2 \sum_{\mu \in A} \sum_{\nu \in B} |P_{\mu\nu}|^2$$

Fulton [21] and Bader [22] proved that benzene has a larger DI in para and meta atoms position. This finding was used by Poater et al. to define the para-delocalization index, which uses DIs of para-related atoms in 6-MRs as a measure of aromaticity. [1]

$$PDI(A) = \frac{\delta(A_1, A_4) + \delta(A_2, A_5) + \delta(A_3, A_6)}{3}$$

For PDI, the larger the index, the greater is the aromaticity. Obviously, this index can only be used for 6-MRs. In this work, it was used to discuss the aromaticity of 6-MRs and the quasi-ring.

4 – Sustainability

In computational chemistry a machine is needed to perform calculations and it obviously requires a certain amount of resources such as electricity, which are mostly obtained from non-sustainable energy sources. To sum up, every time a calculation is executed money is spent and pollution is released, so the amount of calculations and the time required must be reduced to the minimal.

In general, DFT calculations are fast but this can change depending on the molecule. In this case the analysed structures are quite simple, and the number of calculations has been reduced by trying to send just the necessary tests. Also, the time is reduced in different ways, for example, when performing an optimization, the chosen initial geometry is the most similar to the optimised one, reducing the number of steps and the resources required.

Finally, in benefit of computational chemistry regarding the environment, it is very helpful allows lots of possibilities without any usage of toxic reagent or a possible production of waste. This kind of chemistry also prevents the production of many residues because it tells if a certain reaction is possible or not, so it avoids a big quantity of worthless tests in the laboratory.

5 - Results and discussion

In this section, first we will analyse the effect of adding a *quasi*-ring in the benzene as the effect of having an electron-donating group and an electron-withdrawing group (part A). Secondly, enlarging linear topology fused to RAHB will be discussed (part B), first for a total linear systems and second with RAHB in a kink position. Thirdly, total kink topology will be discussed (part C). Lastly, it will be chosen a mix topology to predict the changes in RAHB distances, spin distribution and S-T gap changes (part D).

A. Adding RAHB:

Substituent may effect the molecular electronic structure and its properties: spin density and the excitation energy. The π -electron-donating -OH and the π -electron-accepting -CHO substituents were studied, as they are the substituents that form the *quasi*-ring responsible for the RAHB.

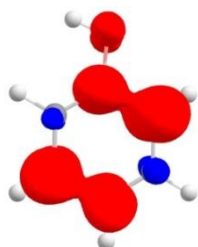


Figure 7. Distribution of spin density of the phenol. Generated with the ChemCraft program.

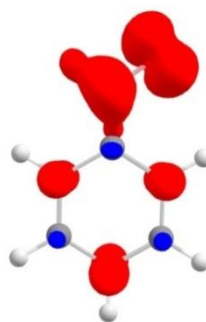


Figure 8. Distribution of spin density of the benzaldehyde. Created with the ChemCraft program.

First, the π -electron-donating -OH group was analysed and S_0 and T_1 were calculated. The excitation energy is 3.6 eV, which matches with the paper [7] that it is 3,6 eV. Spin density distribution in its triplet state is shown in **Figure 7**. As it can be seen, spin density concentrates in the ring and a little bit in the oxygen of the group; that's the reason the excitation energy is lower than the benzene one's (3,8 eV) but not very much.

Then, the π -electron-accepting -CHO group was studied and S_0 and T_1 state were calculated. The excitation energy is 2.9 eV. Spin density distribution in T_1 state is shown in **Figure 8**. As it can be observed, the spin density accumulates in the -CHO group, and very little in the ring. This is the reason that the excitation energy is lower than the benzene (3,8 eV) and the previous result with the -OH group (3.6 eV).

Finally, we substituted the benzene with these two groups together, which resulted of a RAHB between the oxygen of the -OH group and the hydrogen of -CHO group, this will be named *quasi*-ring. In this work we will name our systems HA (hydroxybenzaldehyde).

B. Linear topology:

In the linear topology, the *quasi*-ring has two possibilities of placement: where the *quasi*-ring is in a linear trend (L1) which corresponds to the pink placement in the **figure 9**; and where the *quasi*-ring is in the next possible location (L2) which corresponds to the yellow placement, but we have to take into consideration that there are two isomers: 1 and 2.

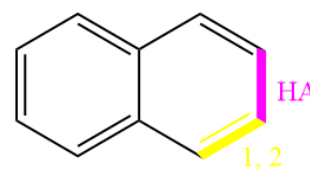


Figure 9. Possible placements for the linear compound. HAx ($x=1-5$) does not have two isomers because of the symmetry. 1 and 2 are the two possible isomers. Figure generated by ChemDraw.

B.1. Linear trend (L1):

First, we analysed the excitation energy and the bond distance for the L1. The name was HA and the number of 6-MRs combined HAx ($x=1-5$):

Table 1. Excitation energies (eV) and bond distances (Å) of the S_0 and T_1 of C=C and O–H for the linear compounds. HAx (where $x=1-5$ 6-MRs).

L1	ΔE_{S-T}	r(O–H)		r(C=C)	
		S_0	T_1	S_0	T_1
HA1	2,37	1,755	0,988	1,419	1,479
HA2	2,19	1,780	1,463	1,437	1,422
HA3	1,52	1,788	1,645	1,446	1,415
HA4	1,03	1,791	1,706	1,451	1,421
HA5	0,67	1,791	1,737	1,453	1,428

In the **table 1**, we can find the excitation energy and the bond distance of O–H and C=C for the S_0 and T_1 for each linear compound. As it can be observed, the excitation energy decrease as the chain lengthens: it goes from 2,37 eV (HA1) to 0,67 eV (HA5). The bond distance of O–H stays the same in the S_0 state, but in the T_1 state increases until it is similar the S_0 state bond length. The bond distance of C=C does not have significant changes. The HA1 suffers an hydrogen transfer from the –OH group to the to the –CHO group, that’s the reason the bond distance of O–H is 0,988 Å.

Then, the spin density and aromaticity were analysed. From the work 8 we could compare the spin density from polybenzenoid hydrocarbons (BPHs) with our compounds:

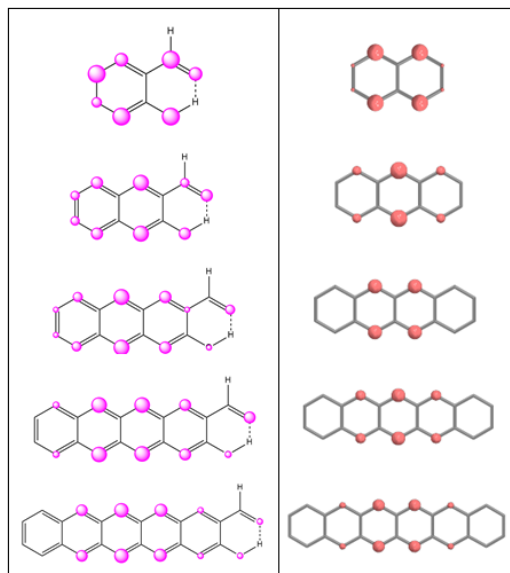


Figure 10. Spin densities of L1 compounds are on the left and spin density of the compounds extracted from paper [8] are on the right.

In the comparative of the spin density, we can see that it is located in the central part of the chain for both cases, so the behaviour of our compounds and the paper are similar. For the HA1 compound, spin density distributes in the 6-MR and in the *quasi*-ring. When the chain lengthens, the spin density is no longer in the *quasi*-ring. This change of the unpaired electrons position helps us explain why, as the change increase, the RAHB bond distances are more similar between S_0 and T_1 , as the excitation takes place far from the *quasi*-ring.

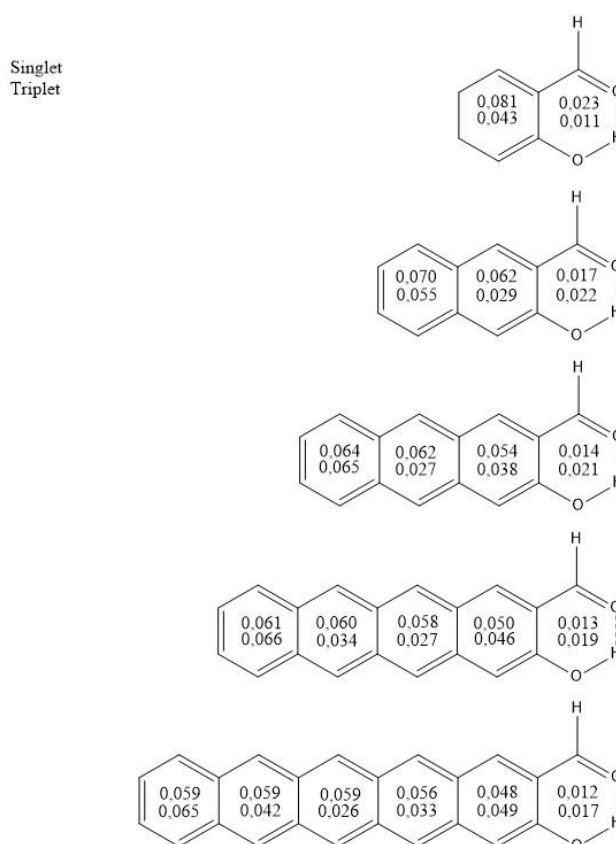


Figure 11. Aromaticity of the L1 compounds was calculated using PDI in S_0 and T_1 for each compound. The S_0 result is the number above and the T_1 result is the number below inside each ring. Figures generated by ChemDraw.

For the aromaticity study, it can be observed that it is distributed in the middle part of the chain as the chain lengthens, this is reflected by the T_1 being reduced compared with the S_0 . It can be seen very clear that as the chain lengthens, the T_1 of the ipso-ring it will be less affected, so for the HA5 the ipso-ring maintains the same aromaticity for both states.

As we have seen for the spin density and the aromaticity, unpaired electrons are in the middle part of the chain. So the longer the chain, the least changes in the RAHB. This is also reflected in the bond distances: as the chain lengthens, S_0 and T_1 look more alike (they are less effected).

B.2. Linear topology for both isomers:

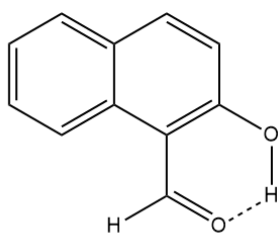


Figure 12. Representation of the isomer 1, which the hydrogen of the $-CHO$ group suffers repulsion with the hydrogen of the ipso-ring. Figure generated by ChemDraw.

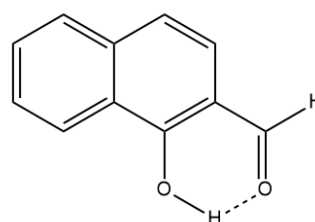


Figure 13. Representation of the isomer 2, which it does not suffer any repulsion. Figure generated by ChemDraw.

We calculated the excitation energy and the bond distance ($O-H$ and $C=C$) for each compound and its isomer:

Table 2. Excitation energies (eV) and bond distances (\AA) of the S_0 and T_1 of $C=C$ and $O-H$ for the L2 compounds. HAx_1 (where $x=2-5$ 6-MRs).

L2	ΔE_{S-T}	r(O--H)		r(C=C)	
		S_0	T_1	S_0	T_1
HA2_1	2,42	1,656	1,619	1,410	1,494
HA3_1	1,88	1,639	1,680	1,405	1,453
HA4_1	1,30	1,630	1,674	1,403	1,430
HA5_1	0,87	1,628	1,662	1,402	1,420

Table 3. Excitation energies (eV) and bond distances (\AA) of the S_0 and T_1 of $C=C$ and $O-H$ for the L2 compounds. HAx_2 (where $x=2-5$ 6-MRs).

L2	ΔE_{S-T}	r(O--H)		r(C=C)	
		S_0	T_1	S_0	T_1
HA2_2	2,38	1,699	1,658	1,404	1,480
HA3_2	1,80	1,679	1,738	1,400	1,444
HA4_2	1,25	1,669	1,723	1,399	1,425
HA5_2	0,83	1,664	1,709	1,398	1,415

As it can be observed, there are two tables: one for the each isomer. In both cases, the excitation energy decreases as long as the chain lengthens, not as much as the previous

compounds (L1). The bond distance O--H and C=C for both states do not vary very much, even with the elongation of the chain; that is a difference from the linear. Moreover, the T_1 is larger than S_0 , which is also a difference from the L1 compounds. The explanation of this difference is related to the common C=C bond length change when going from S_0 and T_1 . While for L1 compounds there is a slightly increase of the C=C double bond character (it shortens), in the present structures this double bond character decrease, bringing to a larger C=C bond length. This is translated to an increase or decrease of the HB bond. For L1 compounds the HB is shorter when it is excited to T_1 while for HAx_1 and HAx_2 is longer.

The differences between the 1 and 2 are due to repulsion; in the isomer 1, the hydrogen of the group -CHO suffers repulsion with the hydrogen from the ipso-ring, this is why HB distances are shorter for isomer 1 than 2. So, the spin density comparative and the aromaticity were analysed only for the isomer 2:

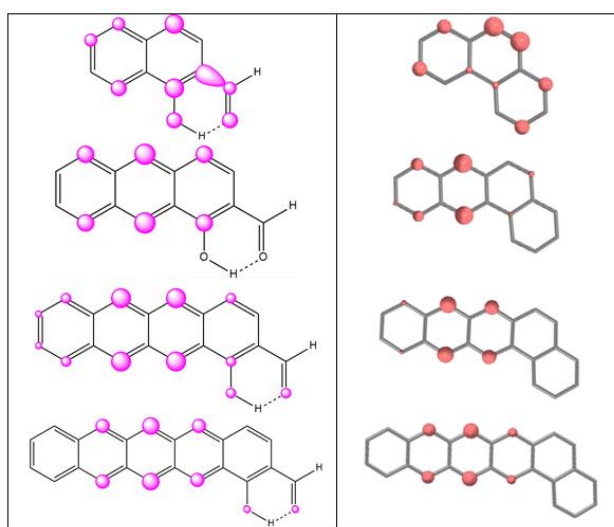


Figure 14. Spin densities of L2 compounds are on the left and spin density of the compounds extracted from paper [8] are on the right. Spin density was analysed only for the isomer 2 (the one who didn't suffer from repulsion).

For the spin density, our compounds follow the same behaviour as the ones of the paper [8]. From the image, it can clearly be observed that the *quasi*-ring acts as a “normal” ring, but with a lightly spin density at the oxygen atoms. For the majority of the compounds, the spin density stays in the middle of the chain; except for the HA2 in which stays at the *quasi*-ring.

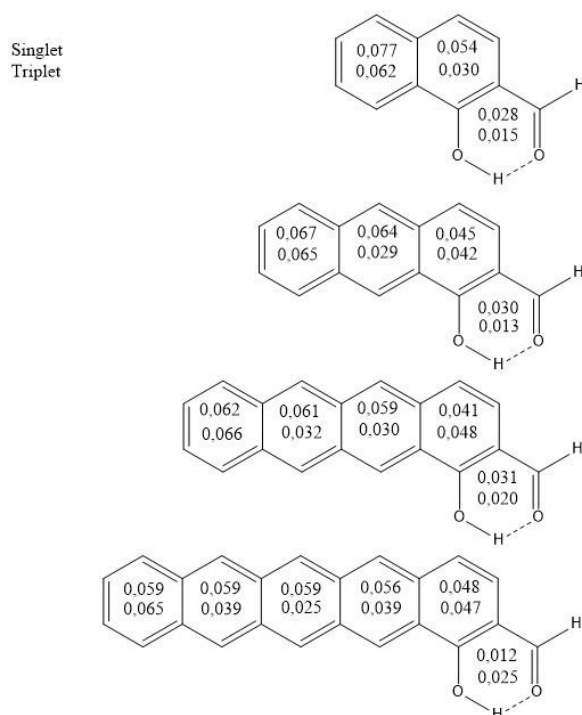


Figure 15. Aromaticity of the L2 compounds was calculated using PDI in S_0 and T_1 for each compound. The S_0 result is the number above and the T_1 result is the number below inside each ring. Figures generated by ChemDraw.

For the aromaticity, as long as the chain lengthens, the T_1 of the ipso-ring it will be less affected (S_0 and T_1 have similar aromaticity).

As we see previously with the L1 compounds, unpaired electrons are in the middle part of the chain. So, as the chain gets longer, fewer changes occur in the bond distance of RAHB (S_0 and T_1 are less affected). This behaviour is similar as L1 compounds for the aromaticity and spin density, but the effect is bigger for the L1 compounds. For the distance bond, L2 compounds the T_1 gets bigger than the S_0 , this is different from the L1 compounds (where the S_0 was bigger than the T_1). HA2 does not follow this, as the spin density and aromaticity concentrate in the *quasi*-ring and this is reflected in the bond distance, which S_0 is smaller than the T_1 .

C. Kink structure for both isomers:

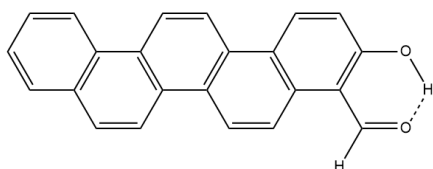


Figure 16. Representation of the isomer 7, which the hydrogen of the $-CHO$ group suffers a repulsion with the hydrogen of the ipso-ring. Figure generated by ChemDraw.

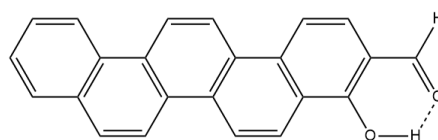


Figure 17. Representation of the isomer 8, which it does not suffer any repulsion. Figure generated by ChemDraw.

The excitation energy and the bond distance (O--H and C=C) for each compound and its isomer were calculated:

Table 4. Excitation energies (eV) and bond distances (Å) of the S_0 and T_1 of C=C and O--H for the kink compounds. HAx_7 (where x=3-5 6-MRs). This isomer suffers repulsion from the hydrogen of the -CHO group with the hydrogen of the ipso-ring.

Kink	ΔE_{S-T}	r(O--H)		r(C=C)	
		S_0	T_1	S_0	T_1
HA3_7	2,51	1,661	1,539	1,413	1,492
HA4_7	2,44	1,660	1,592	1,411	1,489
HA5_7	2,46	1,661	1,575	1,411	1,490

Table 5. Excitation energies (eV) and bond distances (Å) of the S_0 and T_1 of C=C and O--H for the kink compounds. HAx_7 (where x=3-5 6-MRs).

Kink	ΔE_{S-T}	r(O--H)		r(C=C)	
		S_0	T_1	S_0	T_1
HA3_8	2,47	1,711	1,533	1,406	1,476
HA4_8	2,39	1,709	1,619	1,405	1,471
HA5_8	2,41	1,711	1,590	1,405	1,473

Herein, we have the two isomers: the 7 and 8. The isomer 7 suffers repulsion from the hydrogen of the -CHO group and the ipso-ring.

As a general view, the excitation energy does not vary for both isomers. Bond distance is different because of the repulsion of the isomer 7, so the bond distance is shorter than the bond distances of isomer 8. This is an important difference compared to the linear topology. The bond distances do not vary very much and do not follow any tendency.

The spin density and the aromaticity were analysed only for the isomer 8:

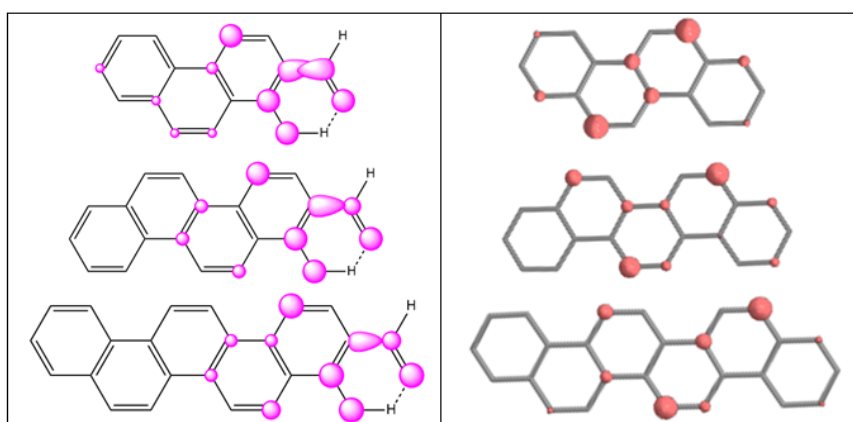


Figure 18. Spin densities of the kink compounds are on the left and spin density of the compounds extracted from paper [8] are on the right. Spin density was analysed only for the isomer 8 (the one who did not suffer repulsion).

For the spin density, as it can be seen these compounds do not follow the same behaviour as the linear compounds nor the paper compounds: the spin density remains in the *quasi*-ring even when the chain lengthens.

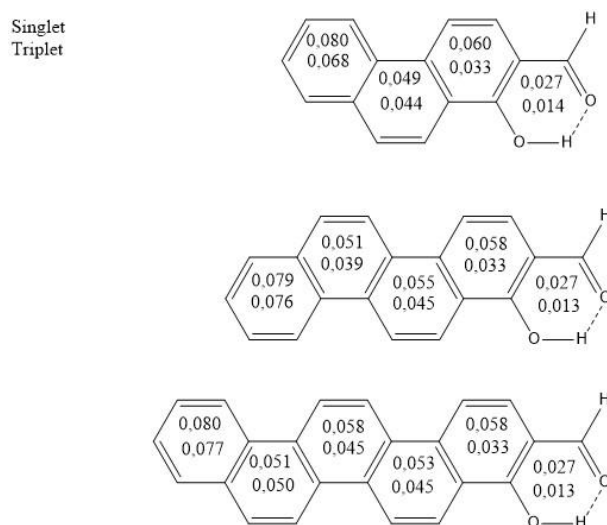


Figure 19. Aromaticity of the kink compounds was calculated using PDI in S_0 and T_1 for each compound. The S_0 result is the number above and the T_1 result is the number below inside each ring. Figures generated by ChemDraw.

For the aromaticity, the ipso-ring stays the same in all cases. These compounds suffer a loss of aromaticity towards quasi-ring. Aromaticity does not suffer variation even with the elongation of the chain. This is why bond distance and excitation energy do not change even in T_1 .

So, for these compounds, there is no noticeable tendency.

D. Combined topology:

From the systems studied above we could see that the behaviour of linear and kink topologies are very different. In linear systems the increase of the number of 6-MR concentrates the spin density at the middle of the chain, so decrease the gap S_0 - T_1 and have less effects of RAHB distances. In kink topologies there were no important changes upon excitation from S_0 and T_1 at the RAHB bond length. These results are similar to the ones found in the paper [8]. Can we predict if there will be changes in RAHB from topology of the different PAHs chains?

The study was made for several compounds. Although the first studies and comparisons were made with linear and kink structures, we also studied more topologies. These topologies were classified by families: family 3 is formed by three 6-MRs and a quasi-ring and can have two different topologies; family 4 is formed by four 6-MRs and a quasi-ring and can have three different topologies; and family 5 is formed by five 6-MRs and a quasi-ring and can have seven different topologies. For each topology there are several possible placements of the quasi-ring and its isomer that can be seen in **figure S1, S2 and S3**.

All these topologies and its bond distance and excitation energy results are in the **table S1**. Although we calculated all these topologies, we did not study them deeply. With an overall view, we can say all topologies follow the behaviour of the linear and kink structure. To support this statement, we studied a topology in which we can see linear and kink stretches.

Further analysis of this topology and its results are shown in **figure 20**. As we said, our main goal here is to predict if the addition of a quasi-ring in different positions will increase or decrease the HB when it will be excited to triplet state. It even can show no changes.

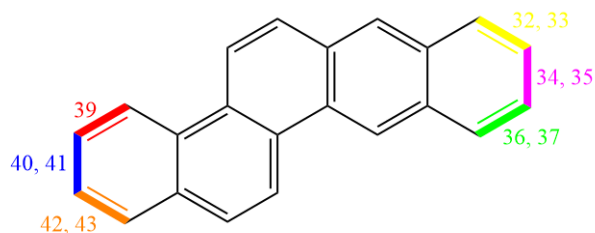


Figure 20. Representation of the topology and its possible placements of the two isomers. The compound 38 was not able to calculate because of repulsion. Figure generated by ChemDraw.

We have six possible placements of the quasi-ring. The analysis was made for the compounds which did not suffer from repulsion: 32, 34, 37, 39, 40 and 42. According to the paper [8] spin will be located in the linear stretch.

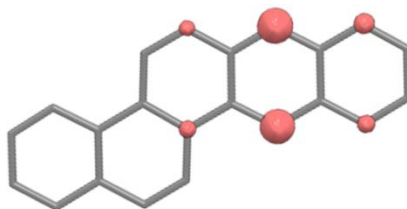


Figure 21. Representation of the spin density for this BPH topology. Figure extracted from the paper [8].

For the placements 32, 34 and 37, we expected that the change between S_0 and T_1 would be larger than for the placements 39, 40 and 42 because of spin density distribution. For the 32, 34 and 37 placements, the excitation energy stays the same for the 32 and 37 (1,89 eV) and for the 34 is lower (1,63 eV). The bond distances of the 32, 34 and 37 compounds are 1,687 Å, 1,784 Å and 1,681 Å for the S_0 and 1,732Å, 1,634Å and 1,727Å for the T_1 , respectively.

However, for the placements of 39, 40 and 42, we expected that the difference between S_0 and T_1 for the bond distance would be very small; because when we excited the molecule, the unpaired electrons stay in the linear stretch of the molecule not the part of 39, 40 and 42. For the three placements, the excitation energy stays the same (1,90 eV, 1,90 eV and 1,94 eV). For the compound 39, 40 and 42, the bond distance of O--H for the S_0 are 1,633 Å, 1,77Å and 1,709 Å and for the T_1 distance are 1,651 Å, 1,750Å and 1,716 Å respectively. As it can be seen, the distance between S_0 and T_1 are very similar.

As it can be proved, this behaviour follows the linear and kink behaviours. The placements 32 and 37 behave as the L2 compounds: the bond distance of the T_1 is bigger than the S_0 ; yet the placement 34 behaves as the L1: the bond distance of the T_1 is smaller than the S_0 .

The placements 39, 40 and 42 kind of follow the behaviour of the kink structure; so there is not a clear tendency. The 40 follows a linear trench that's the reason that the T_1 is smaller than the S_0 , but not in a significant value; and the same happens for the other two structures (39 and 42): the change is not significant and do not follow any tendency.

From all the structures calculated, one can see that they follow similar tendencies to the one presented above, so this allows us to tune the HB distances as well as the S-T gap using different topologies.

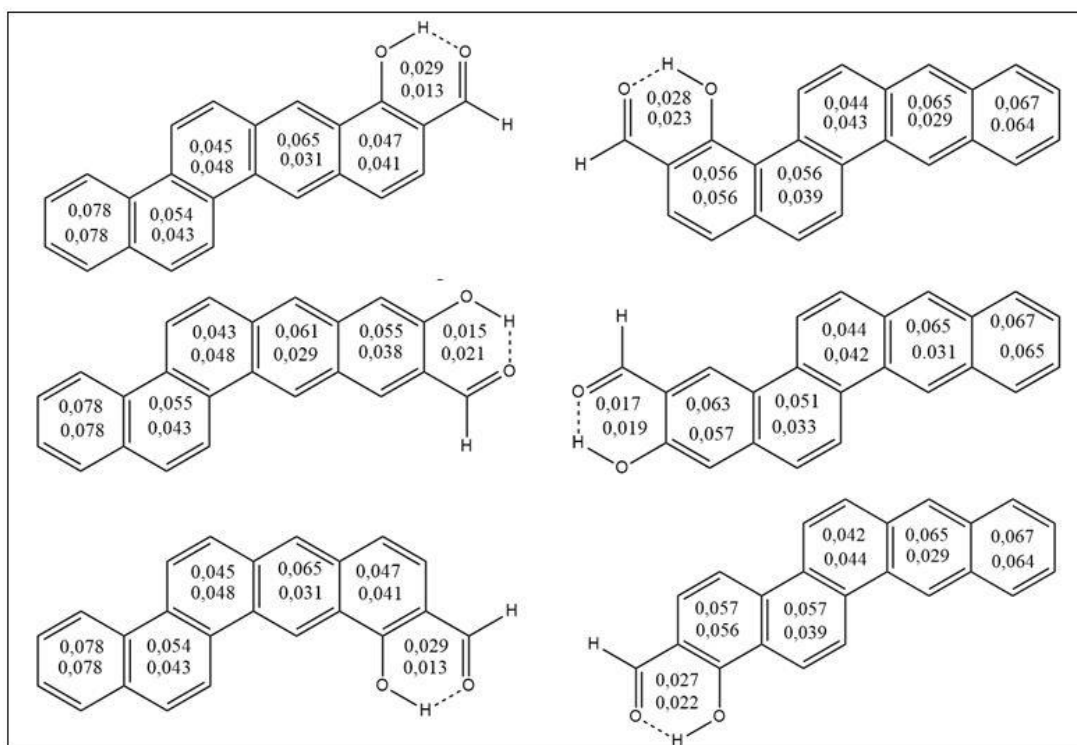


Figure 22. Aromaticity values of the combined topology. PDI was calculated. Figures generated by ChemDraw.

For the aromaticity study, in the **figure 22** one can find the aromaticity (based on PDI indexes) related to all commented possible structures. It is important to check how the aromatic or antiaromatic character depends on the place where the unpaired electrons are localized when going from S_0 to T_1 .

If we analyse the first structure in the **figure 22**, it can be observed that the first ring on the left suffers no changes respect to aromatic character, so no changes are expected when RAHB is placed in that part. The larger changes are allocated in the linear stretch, just as it was expected as it is where the unpaired electrons are placed.

6- Conclusions

After studying the effect of adding a quasi-ring in different topologies we can conclude that:

- For linear topology, spin density and aromaticity follow the same behaviour: as the chain lengthens the unpaired electrons locate in the middle part of the chain. So the longer the chain, the least changes in the RAHB bond distances. S_0 have tendency to be larger than T_1 and when the chain lengthens T_1 increase to get similar values to S_0 .
- For the linear topology with RAHB in a kink position, spin density and aromaticity, the unpaired electrons locate in the middle part of the chain with a lightly spin density at the oxygen atoms, so the RAHB bond distances follow the L1 compounds but do not have that much effect. T_1 have a tendency to be larger than S_0 because of the change in the double bond character of T_1 .
- For kink topology, spin density does not follow the previous behaviour; unpaired electrons locate in the quasi-ring even when the chain lengthens. And for the aromaticity, these compounds suffer a loss of aromaticity towards the quasi-ring and this does not change even with the elongation of the chain. RAHB bond distances and excitation energy do not change even in T_1 . So, for these compounds, there is no noticeable tendency.
- Combined topology allowed us to prove these statements in different structures.

These statements can be very interesting in order to tune the HB distances as well as the S-T gap changing the length of the chain or the topology of the chain for futures studies.

7- Bibliography

1. Pareras, G., Szczepanik, D. W., Duran, M., Solà, M., & Simon, S. (2019). *Tuning the Strength of the Resonance-Assisted Hydrogen Bond in Acenes and Phenacenes with Two o-Hydroxyaldehyde Groups—The Importance of Topology*. *The Journal of Organic Chemistry*, 84(23), 15538–15548. <https://doi.org/10.1021/acs.joc.9b02526>
2. Palusiak, M., Simon, S., & Solà, M. (2006). *Interplay between Intramolecular Resonance-Assisted Hydrogen Bonding and Aromaticity in o-Hydroxyaryl Aldehydes*. *The Journal of Organic Chemistry*, 71(14), 5241–5248. <https://doi.org/10.1021/jo060591x>
3. Gilli, G., Bellucci, F., Ferretti, V. and Bertolasi, V., (1989). *Evidence for resonance-assisted hydrogen bonding from crystal-structure correlations on the enol form of the .beta.-diketone fragment*. *Journal of the American Chemical Society*, 111(3), pp.1023-1028. <https://doi.org/10.1021/ja00185a035>
4. Filarowski, A., Kochel, A., Cieslik, K. and Koll, A., (2005). *Steric and aromatic impact on intramolecular hydrogen bonds in o-hydroxyaryl ketones and ketimines*. *Journal of Physical Organic Chemistry*, 18(10), pp.986-993. <https://doi.org/10.1002/poc.942>
5. Raczyńska, E., Krygowski, T., Zachara, J., Ośmiałowski, B. and Gawinecki, R., (2005). *Tautomeric equilibria, H-bonding and π -electron delocalization in o-nitrosophenol. A B3LYP/6-311 + G(2df,2p) study*. *Journal of Physical Organic Chemistry*, 18(8), pp.892-897. <https://doi.org/10.1002/poc.963>
6. Kaiser, R. I., & Hansen, N. (2021). *An Aromatic Universe—A Physical Chemistry Perspective*. *The Journal of Physical Chemistry A*, 125(18), 3826–3840. <https://doi.org/10.1021/acs.jpca.1c00606>
7. Baranac-Stojanović, M. (2020). *Substituent Effect on Triplet State Aromaticity of Benzene*. *The Journal of Organic Chemistry*, 85(6), 4289–4297. <https://doi.org/10.1021/acs.joc.9b03472>
8. Markert, G., Paenurk, E., & Gershoni-Poranne, R. (2021). *Prediction of Spin Density, Baird-Antiaromaticity, and Singlet–Triplet Energy Gap in Triplet-State Polybenzenoid Systems from Simple Structural Motifs*. *Chemistry – A European Journal*, 27(23), 6923–6935. <https://doi.org/10.1002/chem.202005248>
9. Fluorescence and Phosphorescence. (2020, September 1). Retrieved May 30, 2021, from <https://chem.libretexts.org/@go/page/41400>
10. Pi Molecular Orbitals of Benzene. (2015, July 18). Retrieved May 30, 2021, from <https://chem.libretexts.org/@go/page/32472>

11. Gaussian 16, Revision A.03,
M. J. Frisch, G. W. Trucks, H. B. Schlegel, G. E. Scuseria,
M. A. Robb, J. R. Cheeseman, G. Scalmani, V. Barone,
G. A. Petersson, H. Nakatsuji, X. Li, M. Caricato, A. V. Marenich,
J. Bloino, B. G. Janesko, R. Gomperts, B. Mennucci, H. P. Hratchian,
J. V. Ortiz, A. F. Izmaylov, J. L. Sonnenberg, D. Williams-Young,
F. Ding, F. Lipparini, F. Egidi, J. Goings, B. Peng, A. Petrone,
T. Henderson, D. Ranasinghe, V. G. Zakrzewski, J. Gao, N. Rega,
G. Zheng, W. Liang, M. Hada, M. Ehara, K. Toyota, R. Fukuda,
J. Hasegawa, M. Ishida, T. Nakajima, Y. Honda, O. Kitao, H. Nakai,
T. Vreven, K. Throssell, J. A. Montgomery, Jr., J. E. Peralta,
F. Ogliaro, M. J. Bearpark, J. J. Heyd, E. N. Brothers, K. N. Kudin,
V. N. Staroverov, T. A. Keith, R. Kobayashi, J. Normand,
K. Raghavachari, A. P. Rendell, J. C. Burant, S. S. Iyengar,
J. Tomasi, M. Cossi, J. M. Millam, M. Klene, C. Adamo, R. Cammi,
J. W. Ochterski, R. L. Martin, K. Morokuma, O. Farkas,
J. B. Foresman, and D. J. Fox, Gaussian, Inc., Wallingford CT, 2016.
12. Becke, A., (1993). *Density-functional thermochemistry. III. The role of exact exchange*. The Journal of Chemical Physics, 98(7), pp.5648-5652. <https://doi.org/10.1063/1.464913>
13. Lee, C., Yang, W. and Parr, R., (1988). *Development of the Colle-Salvetti correlation-energy formula into a functional of the electron density*. Physical Review B, 37(2), pp.785-789. <https://doi.org/10.1103/PhysRevB.37.785>
14. Stephens, P., Devlin, F., Chabalowski, C. and Frisch, M., (1994). *Ab Initio Calculation of Vibrational Absorption and Circular Dichroism Spectra Using Density Functional Force Fields*. The Journal of Physical Chemistry, 98(45), pp.11623-11627. <https://doi.org/10.1021/j100096a001>
15. Miehlich, B., Savin, A., Stoll, H. and Preuss, H., (1989). *Results obtained with the correlation energy density functionals of Becke and Lee, Yang and Parr*. Chemical Physics Letters, 157(3), pp.200-206. [https://doi.org/10.1016/0009-2614\(89\)87234-3](https://doi.org/10.1016/0009-2614(89)87234-3)
16. Krishnan, R., Binkley, J., Seeger, R. and Pople, J., (1980). *Self-consistent molecular orbital methods. XX. A basis set for correlated wave functions*. The Journal of Chemical Physics, 72(1), pp.650-654. <https://doi.org/10.1063/1.438955>
17. McLean, A. and Chandler, G., 1980. Contracted Gaussian basis sets for molecular calculations. I. Second row atoms, Z=11–18. The Journal of Chemical Physics, 72(10), pp.5639-5648. <https://doi.org/10.1063/1.438980>
18. Matito, E. ESI-3D: Electron Sharing Indices Program for 3D Molecular Space Partitioning; Institute of Computational chemistry and Catalysis (IQCC), University of Girona, Catalonia, Spain, 2006; <http://iqc.udg.es/eduard/ESI>

19. Matito, E., Duran, M., & Solà, M. (2005). *The aromatic fluctuation index (FLU): A new aromaticity index based on electron delocalization*. *The Journal of Chemical Physics*, 122(1), 014109. <https://doi.org/10.1063/1.1824895>
20. Matito, E., Solà, M., Salvador, P., & Duran, M. (2007). *Electron sharing indexes at the correlated level. Application to aromaticity calculations*. *Faraday Discuss.*, 135, 325–345. <https://doi.org/10.1039/b605086g>
21. Fulton, R. L., & Mixon, S. T. (1993). *Comparison of covalent bond indexes and sharing indexes*. *The Journal of Physical Chemistry*, 97(29), 7530–7534. <https://doi.org/10.1021/j100131a022>
22. Bader, R. F. W., Johnson, S., Tang, T. H., & Popelier, P. L. A. (1996). *The Electron Pair*. *The Journal of Physical Chemistry*, 100(38), 15398–15415. <https://doi.org/10.1021/jp961297j>

8 -Supporting information

Table S1. Excitation energies (eV) and bond distances (Å) of the S_0 and T_1 of C=C and O--H for all the compounds.

		ev	r(O--H)		r(C=C)	
			s	t	s	t
FAMILY 1	HA1	2,37	1,755	0,988	1,419	1,479
FAMILY 2	HA2	2,19	1,780	1,463	1,437	1,422
	HA2_1	2,42	1,656	1,619	1,410	1,494
	HA2_2	2,38	1,699	1,658	1,404	1,480
FAMILY 3	HA3	1,52	1,788	1,645	1,446	1,415
	HA3_1	1,88	1,639	1,680	1,405	1,453
	HA3_2	1,80	1,679	1,738	1,400	1,444
	HA3_3	2,41	1,650	1,571	1,415	1,486
	HA3_4	2,15	1,550	1,535	1,428	1,497
	HA3_5	1,95	1,775	0,991	1,427	1,480
	HA3_6	2,01	1,773	0,990	1,428	1,478
	HA3_7	2,51	1,661	1,539	1,413	1,492
FAMILY 4	HA4	1,03	1,791	1,706	1,451	1,421
	HA4_1	1,30	1,630	1,674	1,403	1,430
	HA4_2	1,25	1,669	1,723	1,399	1,425
	HA4_3	2,23	1,776	1,577	1,430	1,418
	HA4_4	2,20	1,779	1,488	1,429	1,425
	HA4_5	2,33	1,536	1,441	1,429	1,506
	HA4_6	2,29	1,635	1,602	1,415	1,474
	HA4_7	2,44	1,660	1,592	1,411	1,489
	HA4_8	2,39	1,709	1,619	1,405	1,471
	HA4_9	2,08	1,767	1,772	1,425	1,443
	HA4_10	2,04	1,770	1,765	1,424	1,446
	HA4_11	1,99	1,653	1,600	1,418	1,416
	HA4_12	2,00	1,688	1,727	1,402	1,455
	HA4_13	2,08	1,648	1,675	1,407	1,465
	HA4_14	1,74	1,783	1,614	1,442	1,416
	HA4_15	1,72	1,784	1,607	1,442	1,416
	HA4_16	2,06	1,645	1,667	1,407	1,471
	HA4_17	2,00	1,684	1,723	1,402	1,456
	HA4_18	1,98	1,718	1,670	1,409	1,403
	HA4_19	2,00	1,662	1,632	1,415	1,406
FAMILY 5	HA5	0,67	1,791	1,737	1,453	1,428
	HA5_1	0,87	1,628	1,662	1,402	1,420
	HA5_2	0,83	1,664	1,709	1,398	1,415
	HA5_3	1,90	1,777	1,708	1,429	1,479
	HA5_4	2,29	1,775	1,555	1,429	1,022

HA5_5	2,32	1,639	1,600	1,415	1,476
HA5_6	2,31	1,539	1,405	1,429	1,501
HA5_7	2,46	1,661	1,575	1,411	1,490
HA5_8	2,41	1,711	1,590	1,405	1,473
HA5_9	1,44	1,765	1,778	1,424	1,434
HA5_10	1,41	1,766	1,774	1,423	1,435
HA5_11	1,39	1,656	1,622	1,419	1,414
HA5_12	1,43	1,674	1,728	1,399	1,430
HA5_13	1,50	1,635	1,676	1,404	1,435
HA5_14	1,21	1,789	1,689	1,448	1,419
HA5_15	1,20	1,789	1,686	1,448	1,420
HA5_16	0,28	1,636	1,675	1,404	1,436
HA5_17	1,44	1,674	1,729	1,399	1,430
HA5_18	1,36	1,720	1,694	1,410	1,405
HA5_19	1,37	1,663	1,649	1,416	1,409
HA5_20	2,07	1,692	1,709	1,403	1,461
HA5_21	2,16	1,651	1,662	1,408	1,476
HA5_22	1,83	1,780	1,595	1,441	1,416
HA5_23	1,81	1,781	1,585	1,441	1,418
HA5_24	2,12	1,648	1,650	1,408	1,479
HA5_25	2,08	1,689	1,712	1,403	1,462
HA5_26	2,20	1,715	1,653	1,408	1,404
HA5_27	2,21	1,661	1,623	1,414	1,408
HA5_28	2,24	1,769	1,744	1,426	1,437
HA5_29	2,25	1,772	1,657	1,426	1,465
HA5_31	2,16	1,653	1,615	1,417	1,425
HA5_32	1,89	1,687	1,732	1,401	1,446
HA5_33	1,97	1,645	1,678	1,406	1,453
HA5_34	1,63	1,784	1,634	1,444	1,416
HA5_35	1,62	1,785	1,628	1,443	1,417
HA5_36	1,96	1,641	1,672	1,407	1,459
HA5_37	1,89	1,681	1,727	1,402	1,447
HA5_39	1,90	1,633	1,651	1,414	1,421
HA5_40	1,90	1,777	1,750	1,431	1,424
HA5_41	1,88	1,780	1,747	1,430	1,424
HA5_42	1,94	1,709	1,716	1,404	1,411
HA5_43	1,97	1,659	1,665	1,410	1,416
HA5_44	2,22	1,714	1,650	1,408	1,404
HA5_45	2,24	1,660	1,612	1,414	1,407
HA5_46	2,29	1,770	1,745	1,426	1,442
HA5_47	2,26	1,770	1,723	1,425	1,458
HA5_48	2,09	1,554	1,437	1,430	1,439
HA5_49	2,21	1,647	1,596	1,417	1,423

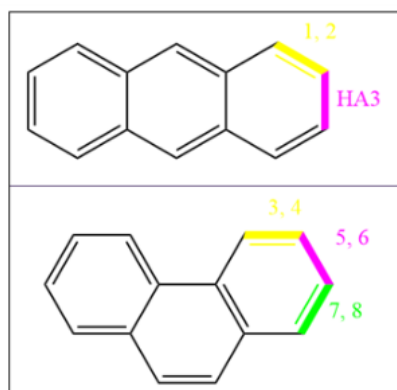


Figure S1. Compounds of the family 3. The colours mark where the quasi-ring can be placed. Figures generated by ChemDraw.

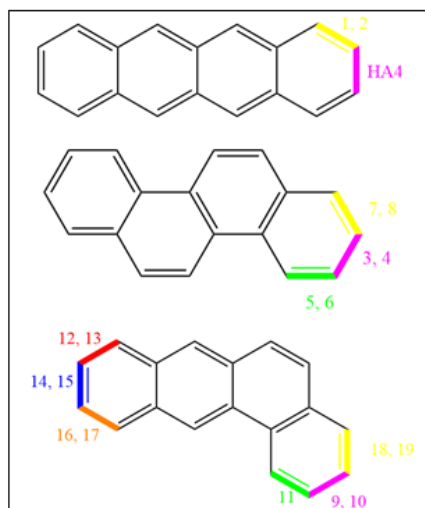


Figure S2. Compounds of the family 4. The colours mark where the quasi-ring can be placed. Figures generated by ChemDraw.

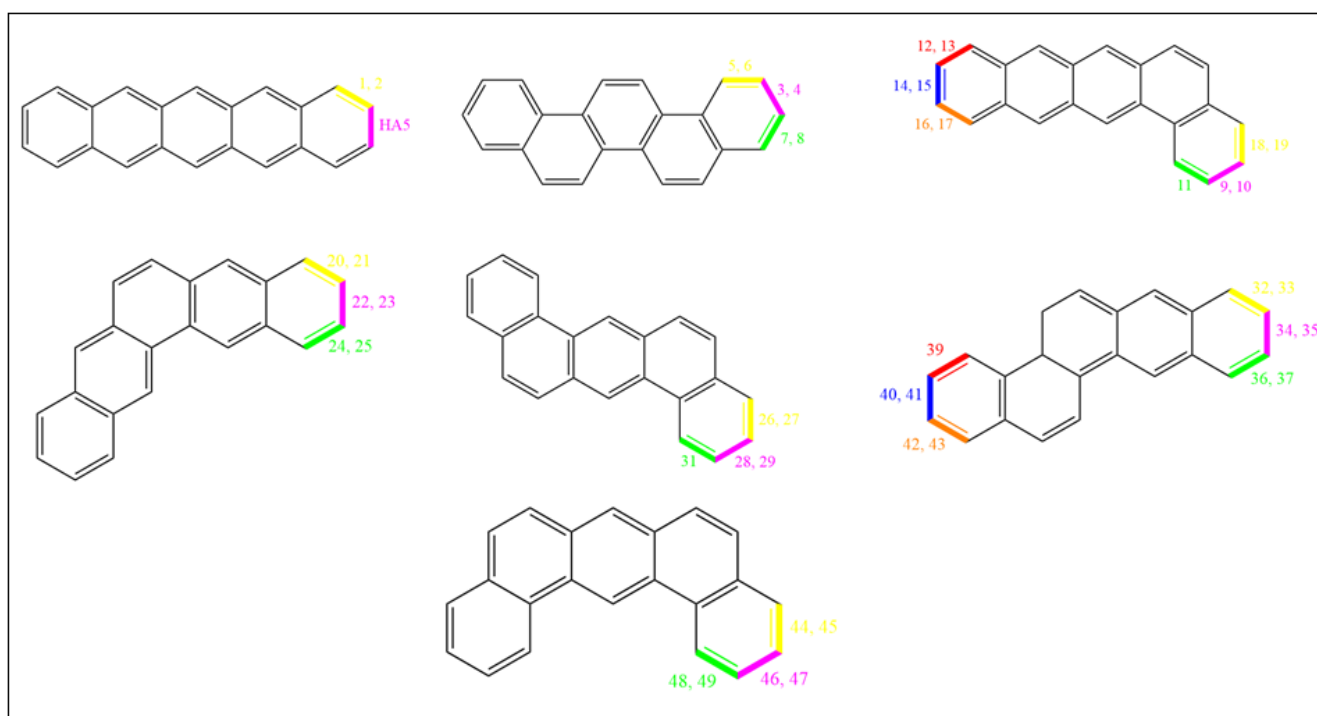


Figure S3. Compounds of the family 5. The colours mark where the quasi-ring can be placed. Figures generated by ChemDraw.